# Spatial scaling of population synchrony in marine fish depends on their life history

Running title: Spatial scaling and life history in fish

Jonatan F. Marquez*, Aline Magdalena Lee, Sondre Aanes, Steinar Engen, Ivar Herfindal, Are Salthaug and Bernt-Erik Sæther

**Jonatan F. Marquez** Centre for Biodiversity Dynamics, Department of Biology, Norwegian University of Science and Technology, 7491 Trondheim, Norway. jonatan.f.marquez@ntnu.no

**Aline Magdalena Lee** Centre for Biodiversity Dynamics, Department of Biology, Norwegian University of Science and Technology, 7491 Trondheim, Norway. lee@alumni.ntnu.no

**Sondre Aanes** Norwegian Computing Center, 0314 Oslo, Norway. sondre.aanes@nr.no

**Steinar Engen** Centre for Biodiversity Dynamics, Department of Mathematical Sciences, Norwegian University of Science and Technology, 7491 Trondheim, Norway. steinar.engen@ntnu.no

**Ivar Herfindal** Centre for Biodiversity Dynamics, Department of Biology, Norwegian University of Science and Technology, 7491 Trondheim, Norway. ivar.herfindal@ntnu.no

**Are Salthaug** Institute of Marine Research, Postbox 1870 Nordnes, 5817, Bergen, Norway. are.salthaug@hi.no

**Bernt-Erik Sæther** Centre for Biodiversity Dynamics, Department of Biology, Norwegian University of Science and Technology, 7491 Trondheim, Norway. bernt-erik.sather@ntnu.no

**Keywords:** abundance, community dynamics, density regulated dispersal, generation time, modifiable areal unit problem, pace of life, population dynamics, population growth rate, slow-fast continuum, spatial processes.

**Article type:** Letters

**Statement of authorship**: BES, SE, IH, SA and AML planned the study. SA and AS collated the data. SA performed the spatial scaling analyses. JFM performed all other statistical

analyses with input from SA and AML. JFM wrote the manuscript with contributions from all other authors.

**Data accessibility statement:** The life history data is available in Bjørkvoll *et al.* (2012), while all the data used in the spatial analyses will be made accessible upon acceptance of the manuscript.

**Number of word in the main text:** 5008

**Number of words in the abstract:** 137

**Number of figures:** 3

**Number of tables:** 1

**Number of references:** 90

**Corresponding author** (*) : Jonatan F. Marquez, Centre for Biodiversity Dynamics, Department of Biology, Norwegian University of Science and Technology, 7491 Trondheim, Norway; Tel.: +47 93040892; e-mail address: jonatan.f.marquez@ntnu.no

## Abstract

The synchrony of population dynamics in space has important implications for ecological processes, for example affecting the spread of diseases, spatial distributions and risk of extinction. Here, we studied the relationship between spatial scaling in population dynamics and species position along the slow-fast continuum of life history variation. Specifically, we explored how generation time, growth rate and mortality rate predicted the spatial scaling of abundance and yearly changes in abundance of eight marine fish species. Our results show that population dynamics of species with “slow” life histories are synchronized over greater distances than those of species with “fast” life histories. These findings provide evidence for a relationship between the position of the species along the life history continuum and population dynamics in space, showing that the spatial distribution of abundance may be related to life history characteristics.

## Introduction

The complexity and scale of spatial population dynamics greatly influence population's responses to current large scale ecological threats, such as climate change, overharvesting and fragmentation (Ellis & Schneider 2008). Population dynamics are mainly regulated by environmental variation and density (Sæther 1997). Because these regulating factors often vary in space, local population parameters (e.g. abundance, vital rates) are also expected to show spatial variation (Barraquand & Murrell 2012). However, the spatial variation of these population parameters is often spatially autocorrelated, meaning that values of population parameters at nearer locations tend to be more similar than at more distant locations (Ellis & Schneider 2008). Similarly, temporal variation in population parameters often correlates more among closer locations than distant ones, resulting in spatial synchrony patterns (Koenig 1999).

The rate at which synchrony in population parameters declines with increased distance (i.e. the spatial scaling) is of central importance in ecology (Engen 2017), for instance because the probability of global extinction increases with increased spatial scaling (Heino *et al.* 1997; Engen *et al.* 2002; Liebhold *et al.* 2004). This is because local densities in synchronized populations are more likely to all be low simultaneously, leaving the entire population vulnerable to stochastic events. Also, synchrony has been shown to influence other ecological processes, such as the rate of spread of invasive species, diseases and parasites (e.g. Ovaskainen & Cornell 2006; Kausrud *et al.* 2007; Giometto *et al.* 2017), the optimal sustainable harvesting rate (e.g. Ruokolainen 2013; Engen 2017), and the relation between occupied range size and population growth rate (Engen 2007). While the presence of spatial synchrony has been established in a variety of systems, identifying drivers causing it has often been more elusive.

Three main processes are known to cause spatial synchrony in population dynamics (Bjørnstad *et al.* 1999; Liebhold *et al.* 2004). First, widely synchrony environmental variables, such as climate, can synchronize dynamics of local populations that have the same density regulation structure (i.e. the Moran effect: Moran 1953; Royama 1977; Grøtan *et al.* 2005). Second, widespread trophic interactions can affect spatial synchrony through, for example, the regulating effects of a common predator/parasite on the vital rates of a prey/host population (Ims & Andreassen 2000). Widespread harvesting can also induce analogous responses in the targeted species (Frank *et al.* 2016; Engen 2017; Engen *et al.* 2018). Third, individual dispersal tends to increase the distance over which population dynamics are synchronized (Ranta 1997; Paradis *et al.* 1999; Bjørnstad & Bolker 2000; Kendall *et al.* 2000). These processes often act simultaneously on a population, hindering the task of quantifying their individual effects, and are further influenced by other factors, such as cyclic population dynamics (Vasseur & Fox 2009) or by geographical patterns (e.g. topography, geographical barriers, latitudinal gradients; Walter *et al.* 2017). Population parameters, like strength of density dependence and demographic stochasticity, have also been shown to affect spatial synchrony, further complicating the identification and understanding of how spatial scaling varies among species (Lande *et al.* 1999; Engen *et al.* 2005b; Sæther *et al.* 2007; Engen 2017).

Theoretical studies have shown how several population parameters, such as strength of density regulation and population growth rate, can affect spatial synchrony (Murdoch *et al.* 1992; Lande *et al.* 1999; Bahn *et al.* 2008). Empirical studies have also identified some important extrinsic factors affecting synchrony in wild populations, such as habitat type (Paradis *et al.* 1999, 2000), weather patterns (Lindström *et al.* 1996; Ranta 1997; Grøtan *et al.* 2005), and harvesting pressure (Frank *et al.* 2016; Kuo *et al.* 2016). However, fewer intrinsic population factors have been studied empirically, with notable exceptions like dispersal strategy (Paradis *et al.* 1999; Jones *et al.* 2007), strength of density regulation and demographic stochasticity among birds (Sæther *et al.* 2007).

Finding general patterns of covariation in ecological processes is important for our understanding of population dynamics and for the development of broad conservation and harvesting strategies. One ecological simplification that has proven to be very useful is the slow-fast continuum of life histories (Jennings *et al.* 1998; Ferguson & Lariviere 2002; Engen *et al.* 2005a; Jones *et al.* 2008). Early maturing species with short generation times and high reproductive rates characterize the fast end of the continuum, while long-lived species with high adult survival represent the slower end (Sæther & Bakke 2000; Ferguson & Lariviere 2002; Oli 2004). From a species' allocation along the continuum (i.e. pace of life), other aspects of its population dynamics can be predicted (Sæther *et al.* 1996; Jennings *et al.* 1998; Jones *et al.* 2008). For example, population growth of faster lived species tends to be more sensitive to changes in fecundity rates, whereas slow lived species are more affected by changes in adult survival (Oli 2004). This general pattern has been demonstrated in wild populations of birds (Sæther & Bakke 2000), mammals (Oli 2004; van de Kerk *et al.* 2013), reptiles (Shine & Charnov 1992; Clobert *et al.* 1998) and fish (Bjørkvoll *et al.* 2012; Thorson *et al.* 2017), and shown to be useful for the development of management strategies (Ferguson & Lariviere 2002).

In this paper we examine whether the pace of life of a species, i.e., its placement along the slow-fast continuum, can also predict the spatial scaling of its population synchrony. We do this by analysing spatial synchrony in two population variables – abundance and yearly change in abundance – in relation to species life history parameters that are directly related to the slow-fast continuum – population growth rate, mortality and generation time – of eight species of fish in the Barents Sea living under similar environmental conditions.

## Materials and Methods

### *Study area*

We used spatial data and life history trait data from eight Barents Sea round-fish species (Fig. 1). Many of the fish stocks in the Barents Sea have been regularly monitored for decades resulting in consistent high-quality datasets with spatial information (Stiansen *et al.* 2008) on species living in the same environment but covering a range of life history strategies (Bjørkvoll *et al.* 2012), making the region an outstanding model to study general patterns of spatial synchrony in relation to life history. The Barents Sea is highly seasonal, becoming largely covered during the winter period by sea ice that gradually melts during spring. Many of the fish inhabiting this sea carry out long seasonal migrations between spawning and feeding grounds (Olsen *et al.* 2010), suggesting high dispersal capabilities. Because spawning occurs largely outside of the study area and is followed by a planktonic phase (Olsen *et al.* 2010), we assume that populations give rise to synchrony through dispersal dynamics and local mortality rates, rather than self-recruitment. In other words, as local abundances fluctuate, local mortality and dispersal dynamics will be affected by density regulation processes thereby affecting abundance distribution patterns, while high reproductive rates at a specific region will not necessarily cause that region, or nearby ones, to receive a greater recruitment in the future. Nevertheless, social learning from older cohorts to younger ones has been suggested for species like herring (*Clupea harengus*; Huse 2016) and capelin (*Mallotus villosus*; Fauchald *et al.* 2006), where older cohorts lead younger ones to particular regions based on experience. This behaviour is reportedly strengthened with the abundance of the older cohort, thereby drawing an indirect link between local abundances of consecutive years. The species included in this study were: North East Atlantic (NEA) cod (*Gadus morhua)*, NEA haddock (*Melanogramus aeglefinus)*, NEA saithe (*Pollachius virens)*, beaked redfish (*Sebastes mentella)*, golden redfish (*Sebastes marinus)*, blue whiting (*Micromesistius poutassou)*, Barents Sea capelin and Norwegian spring-spawning herring. All these species are subject to direct or indirect harvesting (ICES 2016).

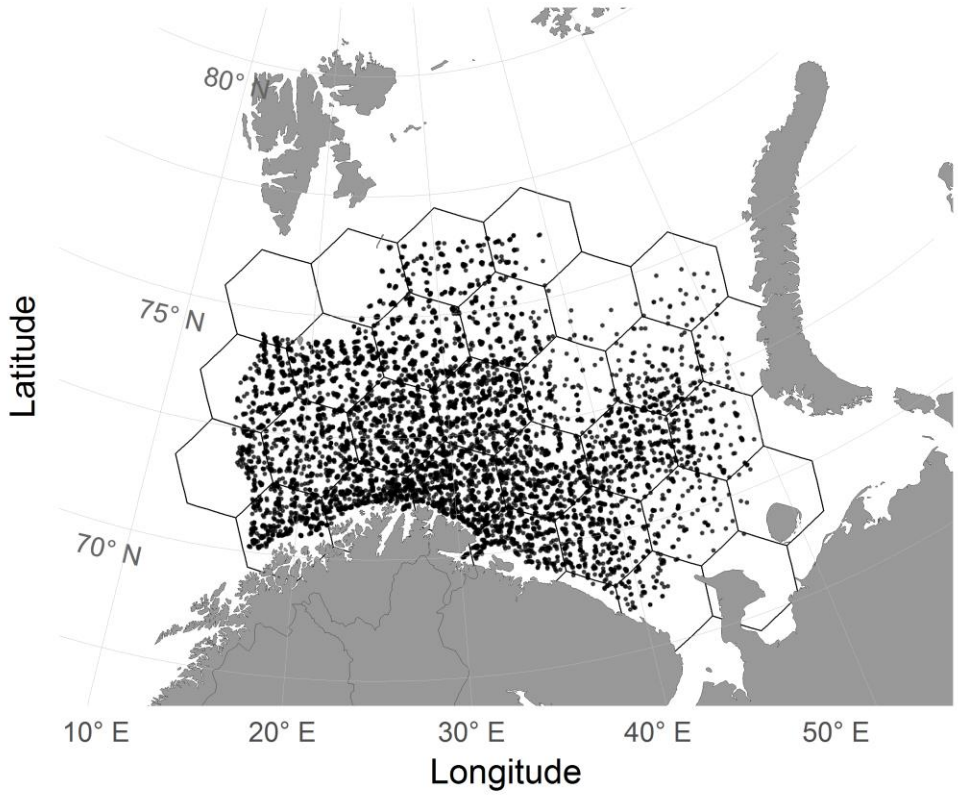


166

167 *Figure 1. Barents Sea and surrounding land masses. The study region is overlaid with the*
168 *hexagonal grid with 36100 km$^2$ cells used in the spatial synchrony analysis. Each dot*
169 *represents a sampling event.*

170

171 ***Estimation of population life history parameters***

172 We used five life history parameters to characterize the species' allocation along the slow-fast
173 continuum; population growth rate and its variability, mortality and its variability, and
174 generation time. Species at the fast end of the continuum are expected to have high population
175 growth rates, high mortality and short generation times (Sæther *et al.* 1996). Fast species are
176 also generally expected to have more variable population dynamics than those at the slow
177 end of the continuum (Shelton & Mangel 2011; Bjørkvoll *et al.* 2012). We therefore also
178 included measures of variability of population growth and mortality. Estimates of life history

parameters were retrieved from Bjørkvoll *et al.* (2012), where they were estimated in a Bayesian hierarchical state-space population model using data on commercial harvesting, scientific survey abundance indices and information on proportions of mature individuals at age per year (ICES 2008a, b, 2009). Detailed information of the data from Bjørkvoll *et al.* (2012) can be found in Appendix 1 and in their supplementary materials.

Generation time ($GT$) was defined as the mean age of mothers of newborn individuals, assuming a stable age distribution. Mortality was estimated as the expected natural mortality rate across ages and years, $\mathrm{E}(M_{a,t})$, starting from the age at which individuals are recruited into the fishery and excluding the mortality caused by harvesting (for a full description of their methodology see Appendix 1 and Aanes *et al.* (2007); Bjørkvoll *et al.* (2012)). The variance of mortality, $\mathrm{Var}(M_{a,t})$, was estimated using the standard formula for the variance of the log-normal distribution. The annual multiplicative population growth rate, $\lambda_t$, represented the potential population growth in the absence of harvesting. Variation in the growth rate among years was included by calculating the coefficient of variation, $\mathrm{CV}(\lambda_t)$.

We used pairwise Pearson correlation tests to confirm that the relationships between these life history parameters corresponded to those expected from life history theory. We expected $GT$ to increase with decreased $\mathrm{E}(M_{a,t})$ and $\lambda_t$, indicating a transition from the fast end to the slow end of the continuum among the species examined. We also expected the $\mathrm{Var}(M_{a,t})$ and $\mathrm{CV}(\lambda_t)$, to increase with increasing $\mathrm{E}(M_{a,t})$ and $\lambda_t$, respectively.

***Estimation of spatial scaling and population synchrony***

The spatial scaling of population variables was estimated using data from scientific bottom trawl surveys performed annually by the Norwegian Institute for Marine Research and the Polar Research Institute of Marine Fisheries and Oceanography from January to March, from 1985 to 2016 (Jakobsen *et al.* 1997; Aanes & Vølstad 2015). The survey followed a stratified

206 sampling design with approximately uniform distribution of sampled locations in space and
207 was, with few exceptions, performed using Campelen 1800 demersal survey trawls with mesh
208 sizes of 22 mm in the codend that were towed for ~30 minutes at a speed of 3 knots and an
209 effecting height of ~4 m (3.5 – 5 m; Aglen 1996). The area covered by the trawls and the
210 geometry of the trawls (i.e. door spread, mouth opening, relative velocity and contact with the
211 bottom) were monitored with doppler logs or GPS and SCANMAR system, respectively. For
212 more details see: Jakobsen *et al.* (1997), Johannesen *et al.* (2009) and Pennington *et al.*
213 (2011).
214
215 The survey data were used to estimate site-specific indices of abundance and yearly change
216 in abundance. A site is defined as each of the cells of hexagonal grids placed over the study
217 region. Yearly changes in abundance are defined as changes in local abundance from a given
218 year to the next and are expected to be driven by fish returning or remaining around the same
219 regions after undergoing spawning migrations, and thereafter influenced by dispersal
220 dynamics, density regulation and mortality rates. To assess the influence of the spatial
221 resolution of the hexagonal grid on the spatial synchrony estimates, we estimated indices of
222 abundance and yearly changes in abundance over cell sizes of 2500, 4900, 8100, 12100,
223 16900, 22500, 28900, 36100 (Fig. 1), 44100 and 52900 $km^2$. The 36100 $km^2$ resolution was
224 chosen for this study based on a balance between minimizing the number of incomplete series
225 and reducing the risk of losing spatial signalling for all species included in this study. Results
226 from the analysis using other resolutions are presented in the supplementary materials
227 (Appendix 2). For simplicity, we performed the spatial analyses under the assumption that
228 distance decay is isotropic. It is possible that underlying spatial heterogeneity could cause
229 different rates of decay in different directions in some cases, but there is no reason to believe
230 that this assumption would cause systematic biases.
231
232 Catch numbers divided by the area swept by the trawl were considered to be direct
233 observations of density (c.f. Aanes & Vølstad 2015), and local densities ($N$) were estimated

by averaging the sampled densities per cell area and year. Local changes in abundance at time t were defined as the log of the ratio of abundance in subsequent years, i.e. $r_t = \log(N_{t+1}/N_t)$. The resulting estimates of log abundance ($\log(N_t)$) and the log of annual changes in abundance ($r_t$) were compiled into time series for each grid-cell. Values of $N_t$ that were 0 were omitted from the analysis as they will result in undefined values of both $\log(N_t)$ and $r_t$, and hence all results are conditioned on $N_t > 0$.

Spatial autocorrelation in the variables $\log(N)$ and $r$ were each estimated with a model where the data are assumed spatially dependent but independent in time, following principles for introducing spatial dependence (see e.g. Cressie & Wikle 2011). For the variable of interest at site $\boldsymbol{s}$ and time $t$, $y(\boldsymbol{s}, t)$, we write

$$y(\boldsymbol{s}, t) = \kappa(\boldsymbol{s}) + W(\boldsymbol{s}, t) + \varepsilon(\boldsymbol{s}, t) \quad (1)$$

where $\kappa(\boldsymbol{s})$ is the mean at site $\boldsymbol{s}$, $W(\boldsymbol{s}, t)$ is a spatially dependent and $\varepsilon(\boldsymbol{s}, t)$ a spatially independent, both zero mean, random variables. Then $W(\boldsymbol{s}, t)$ includes the spatially structured deviations from the mean and $\varepsilon(\boldsymbol{s}, t)$ the residual variability representing microscale and sampling variability. The covariance function of spatial distance $d$ is defined as

$$C_W(d) = \mathrm{Cov}\big(W(\boldsymbol{s}, t), W(\boldsymbol{r}, t)\big) = \sigma(\boldsymbol{s})\sigma(\boldsymbol{r})\rho_Y(d) \quad (2)$$

where $\sigma(\boldsymbol{s})$ is the variance at site $\boldsymbol{s}$, $\rho_Y(d) = [\rho_\infty + (\rho_0 - \rho_\infty)h(d)]$ is the spatial autocorrelation at distance $d$, where $\rho_\infty$ and $\rho_0$ are the correlations of the population variables at infinity and zero distance, respectively. The spatial dependence is captured by $h(d) = exp\left(-\frac{d^2}{2l^2}\right)$, which is a Gaussian function where the parameter $l$ defines the spatial scaling. The residual variation is included in $\varepsilon$ and is independent of $W(\boldsymbol{s}, t)$, such that

$$C_Y(d) = \mathrm{Cov}\big(Y(\boldsymbol{s}, t), Y(\boldsymbol{r}, t) | \kappa(\boldsymbol{s}), \kappa(\boldsymbol{r})\big) = \mathrm{Cov}\big(W(\boldsymbol{s}, t), W(\boldsymbol{r}, t)\big) + \sigma_\varepsilon^2 \mathrm{I}(d = 0) \quad (3)$$

Assuming $\sigma(\boldsymbol{s}) = \sigma(\boldsymbol{r}) = \sigma$, i.e. variance is equal across space, we get the covariance function

$$C_Y(d) = \sigma^2[\rho_\infty + (\rho_0 - \rho_\infty)h(d)] + \sigma_\varepsilon^2 \mathrm{I}(d = 0) \quad (4)$$

Writing $\boldsymbol{Y}_t = \left(Y(\boldsymbol{s}_1, t), Y(\boldsymbol{s}_2, t), \ldots, Y\left(\boldsymbol{s}_{n_s}, t\right)\right)'$, $n_\mathrm{s}$ being the number of sites, we have $\mathrm{E}(\boldsymbol{Y}_t|\boldsymbol{\kappa}) = \boldsymbol{\kappa}$ and $\mathrm{Var}(\boldsymbol{Y}_t|\boldsymbol{\kappa}) = \boldsymbol{\Sigma} + \sigma_\varepsilon^2\mathbf{I}$ where the elements in $\boldsymbol{\Sigma}$ are defined by $\mathrm{Cov}\big(W(\boldsymbol{s}, t), W(\boldsymbol{r}, t)\big)$. Assuming all $W$ and $\varepsilon$ follow lognormal distributions, it may then be shown that the mean corrected values are approximately multivariate normally distributed

$$\mathbf{y}(t) - \widehat{\boldsymbol{\kappa}} \dot{\sim} MVN(0, \boldsymbol{\Sigma} + \sigma_\varepsilon^2\mathbf{I}) \quad (5)$$

where $\widehat{\boldsymbol{\kappa}}$ is the vector of mean values at each location. Hence, the likelihood function $L(\mathbf{y}(t) - \widehat{\boldsymbol{\kappa}}; \theta) = \prod_{t=1}^{T} f(\mathbf{y}(t) - \widehat{\boldsymbol{\kappa}}|\theta)$ is completely specified, such that the parameters $\rho_0, \rho_\infty, \sigma^2$ and $l$ can be estimated by numerical optimization. Distributions of parameters are obtained by non-parametric bootstrapping achieved by resampling vectors of annual $\boldsymbol{Y}_t$ with replacement and subsequently fitting the model to each replicate dataset.

Generalized Linear Models (GLMs) were used to analyse the relationship between each life history trait and scaling of synchrony (i.e. $l$ in the Gaussian function, $h(d)$) of abundance and yearly changes in abundance, independently. Estimates of spatial scaling were log-transformed to linearize their relationship with the life history parameters. First, we used GLMs of the form $\log(Z) = \beta_0 + \beta_1 X$, where the response variable, $Z$, is the spatial scaling parameters $l_{\log(N)}$ or $l_r$, $\beta_0$ is the intercept of the model, $X$ represents one of the life history parameters ($GT$, $\mathrm{E}\big(M_{a,t}\big)$, $\mathrm{Var}\big(M_{a,t}\big)$, $\lambda_t$ or $\mathrm{CV}(\lambda_t)$) and $\beta_1$ represents the rate at which the spatial scaling changes in response to unit changes in the life history traits. The spatial scaling parameter was represented by the median of the distribution of synchrony scalings obtained through a bootstrapping. To account for the heteroskedasticity and non-normality of the variables, we bootstrap-resampled the model 50 000 times using random values from each of

the models' variables. This resulted in 50 000 slope and intercept estimates for each of the ten models. Lastly, to examine the presence of a general relationship between spatial scaling and life history traits, we measured the proportion of positive or negative slopes within the resulting model outputs. All data analyses were carried out in R version 3.5.0 (R Core Team 2018).

*Table 1. Estimated spatial scaling ($l$) of abundance ($log\ (N)$) and annual change in abundance ($r$) with corresponding 95% confidence intervals in brackets, as well as the estimated values for each life history trait obtained from Bjørkvoll et al. (2012) with their 95% credible intervals.*

| | $l$ (km) | |
|---|---|---|
| Species | $\log(N)$ | $r$ |
| Golden redfish | 501.8 (317.2, 803.2) | 352.2 (7.5, 569.5) |
| Beaked redfish | 363.0 (124.0, 613.4) | 141.3 (103.2, 375.4) |
| NSS herring | 247.3 (181.0, 320.6) | 221.7 (6.6, 355.4) |
| NEA saithe | 306.3 (84.9, 504.6) | 30.7 (3.7, 212.01) |
| NEA cod | 279.4 (144.4, 414.5) | 375.1 (202.7, 496.2) |
| NEA haddock | 198.7 (138.0, 308.8) | 270.4 (132.9, 426.5) |
| Blue whiting | 218.7 (165.1, 343.5) | 391.4 (212.8, 573.9) |
| Barents Sea capelin | 201.7 (139.0, 273.3) | 118.5 (12.1, 205.5) |

| | Population parameteres estimates from | | | | |
|---|---|---|---|---|---|
| Species | $GT$ | $\lambda_t$ | $\mathrm{CV}(\lambda_t)$ | $\mathrm{E}(M_{a,t})$ | $\mathrm{Var}(M_{a,t})$ |
| Golden redfish | 14.686 (14.233, 15.143) | 0.974 (.958, .989) | 0.026 (.017, .043) | 0.031 (.007, .079) | 0.001 (.000, .003) |
| Beaked redfish | 14.273 (13.975, 14.499) | 1.032 (1.009, 1.054) | 0.154 (.114, .250) | 0.065 (.010, .149) | 0.005 (.000, .030) |
| NSS herring | 6.793 (6.438, 7.161) | 1.138 (1.093, 1.201) | 0.290 (.175, .448) | 0.254 (.150, .388) | 0.270 (.035, 1.204) |
| NEA saithe | 6.652 (6.291, 7.072) | 1.106 (1.056, 1.169) | 0.235 (.144, .394) | 0.244 (.067, .447) | 0.027 (.001, .111) |
| NEA cod | 6.592 (6.39, 6.737) | 1.212 (1.163, 1.259) | 0.342 (.232, 0.495) | 0.336 (.153, .578) | 0.042 (.010, .103) |
| NEA haddock | 5.757 (5.447, 6.05) | 1.332 (1.260, 1.411) | 0.560 (.434, .725) | 0.424 (.243, .640) | 0.109 (.036, .287) |
| Blue whiting | 4.110 (3.920, 4.283) | 1.346 (1.250, 1.438) | 0.307 (.214, .462) | 0.250 (.051, .485) | 0.034 (.001, .122) |
| Barents Sea capelin | 2.644 (2.312, 3.050) | 1.597 (1.267, 2.241) | 1.033 (.643, 1.841) | 0.508 (.034, 1.204) | 0.273 (.000, 1.362) |

## Results

### *Life history strategies*

As expected, generation times, $GT$, were negatively correlated with expected natural mortality rates at age and year, $\mathrm{E}(M_{a,t})$ (Pearson's r $(R_p)$ = -0.89, n = 8, p = 0.003), and with annual multiplicative population growth rates, $\lambda_t$ ($R_p$ = -0.85, n = 8, p = 0.007). Correspondingly, $\mathrm{E}(M_{a,t})$ and $\lambda_t$ were positively correlated ($R_p$ = 0.89, n = 8, p = 0.003). In this study, capelin, blue whiting and haddock represented the faster end of the continuum, while beaked redfish and golden redfish represented the slow end (Table 1).

The CV of population growth rate, $\mathrm{CV}(\lambda_t)$, were positively correlated with $\lambda_t$ ($R_p$ = 0.94, n = 8, p < 0.001), but negatively with $GT$ ($R_p$ = -0.74, n = 8, p = 0.037). On the other hand, variance in mortality, $\mathrm{Var}(M_{a,t})$, was not significantly correlated with $\mathrm{E}(M_{a,t})$($R_p$ = 0.64, n = 8, p = 0.089), nor with $GT$ ($R_p$ = -0.56, n = 8, p = 0.145).

### *Spatial scaling of abundance and yearly change in abundance*

The scaling estimates of abundance varied markedly among species, more than doubling in distance from the shortest (capelin and haddock) to the longest (golden redfish; Table 1). Increasing the cell sizes of the grid used to calculate spatial synchrony generally increased the estimated spatial scaling of abundance for all species. Coarser resolutions also reduced the uncertainty of the estimates for species with less spatial data that showed high uncertainty at finer resolutions, e.g. Saithe (Appendix 2). We present the results from the analysis performed at a resolution of 36100 km$^2$. This resolution represents a good balance between fine spatial resolution and minimizing noise/error in the abundance estimates. Scaling estimates of yearly changes in abundance differed inconsistently from the scaling estimates of abundance, being in some cases greater and in other cases shorter for different species (Table 1). Varying the resolution influenced the scaling estimates in an inconsistent matter,

although courser resolution generally reduced the overall uncertainty of the estimate (Appendix 2).

***Life history strategy and spatial scaling***

We found a higher spatial scaling of abundance (i.e., synchrony over larger distances, $l_{\log(N)}$) in species with slower life histories. This trend was consistent across the resolutions used in the spatial synchrony analysis. Uncertainty in the estimated relationship decreased with coarser resolutions (Appendix 2). No significant correlation was found between the spatial scaling of yearly change in abundance, $l_{\mathrm{r}}$, and life history strategy regardless of the spatial resolutions examined.

We found a positive relationship between species' generation time, $GT$, and $l_{\log(N)}$ ($\beta_{GT,N}$ = 0.066, 95% CI = (0.041, 0.090), p = 0.002; Fig. 2a). The positive relationship was persistent when accounting for the variance within both variables, as 98.7% of the slopes from the bootstrap were positive. Increasing population growth, $\lambda_t$, predicted a decline in $l_{\log(N)}$ ($\beta_{\lambda,N}$ = -1.351, 95% CI = (-2.011, -0.689), p = 0.007), also evident when accounting for the uncertainty in the variables as 98.7% of the slopes supported a negative correlation (Fig. 2b). A negative pattern was also present in the relationship between $\mathrm{CV}(\lambda_t)$ and $l_{\log(N)}$ ($\beta_{\mathrm{CV}(\lambda),N}$ = -0.786, 95% CI = (-1.324, -0.247), p = 0.029), where 98.6% of the bootstrapped models predicted a negative relationship (Fig. 2c). Expected mortality rate, $\mathrm{E}(M_{a,t})$, showed significant negative correlation with in $l_{\log(N)}$ ($\beta_{\mathrm{E}(M),N}$ = -1.770, 95% CI = (-2.520, -1.012), p = 0.003), with 97% of the bootstrapped models supporting the relationship (Fig. 2d). The relationship between the species' average estimated $\mathrm{Var}(M_{a,t})$ and the median of their estimated $l_{\log(N)}$ values showed a negative trend as well, although non-significant ($\beta_{\mathrm{Var}(M),N}$ = -2.11, 95% CI = (-4.162, -0.064), p = 0.090). The bootstrap-resampling of the model indicated that 94.1% of the models between $\mathrm{Var}(M_{a,t})$ and $l_{\log(N)}$ instances supported a negative relationship (Fig. 2e)

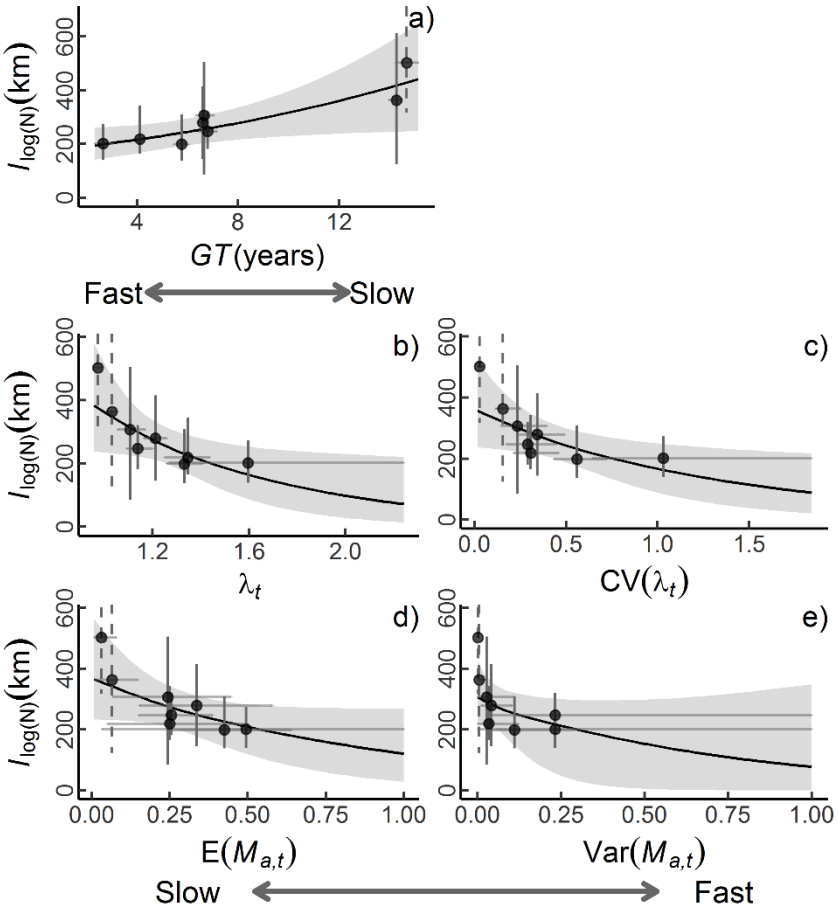


*Figure 2. Relationship between spatial scaling of abundance, $l_{log\ (N)}$, and a) generation time, $GT$, b) multiplicative population growth rate, $\lambda_t$, c) CV of the multiplicative population growth rate, $CV(\lambda_t)$, d) expected mortality rate, $E(M_{a,t})$ and e) variance of mortality, $Var(M_{a,t})$. Points represent the median of each species' spatial scaling estimates and their estimated life history traits, with the vertical and horizontal lines indicate their 95% confidence intervals and credible intervals, respectively. The dashed lines should reach (from left to right) 803 and 613 km, but the range of the y-axis was delimited. The regression line shows the model's prediction with the uncertainty shown by the 95% credible sets in grey. The arrow under the x axis indicates the direction of the relationship between the life history traits and the slow-fast continuum.*

The $GT$ of a species was not found to be correlated with $l_{\mathrm{r}}$ ($\beta_{GT,r}$= 0.02, 95% CI = (-0.136, 0.172), p = 0.826), even when accounting for the variance within both variables in the

bootstrap approach (P ($\beta_1$<0= 0.48); Fig. 3a). Likewise, $l_\mathrm{r}$ was not found to be dependent on $\lambda_t$ ($\beta_{\lambda,r}$ = 0.164, 95% CI = (-3.232, 3.559), p = 0.928; P($\beta_1$<0= 0.483); Fig. 3b), nor dependent on the population's $\mathrm{CV}(\lambda_t)$ ($\beta_{\mathrm{CV}(\lambda),r}$ = -0.798, 95% CI = (-2.414, 4.009), p = 0.644; P($\beta_1$<0= 0.484); Fig. 3c). Finally, neither $\mathrm{E}(M_{a,t})$ nor $\mathrm{Var}(M_{a,t})$ were found to be predictors of variation in $l_\mathrm{r}$ ($\beta_{\mathrm{E}(M),r}$ = -0.356, 95% CI = (-4.647, 3.934), p = 0.876; P($\beta_1$<0= 0.59); $\beta_{\mathrm{Var}(M),r}$ = -0.4214, 95% CI = (-7.534, 6.691), p = 0.911; P($\beta_1$<0= 0.54); Fig. 3d-e)

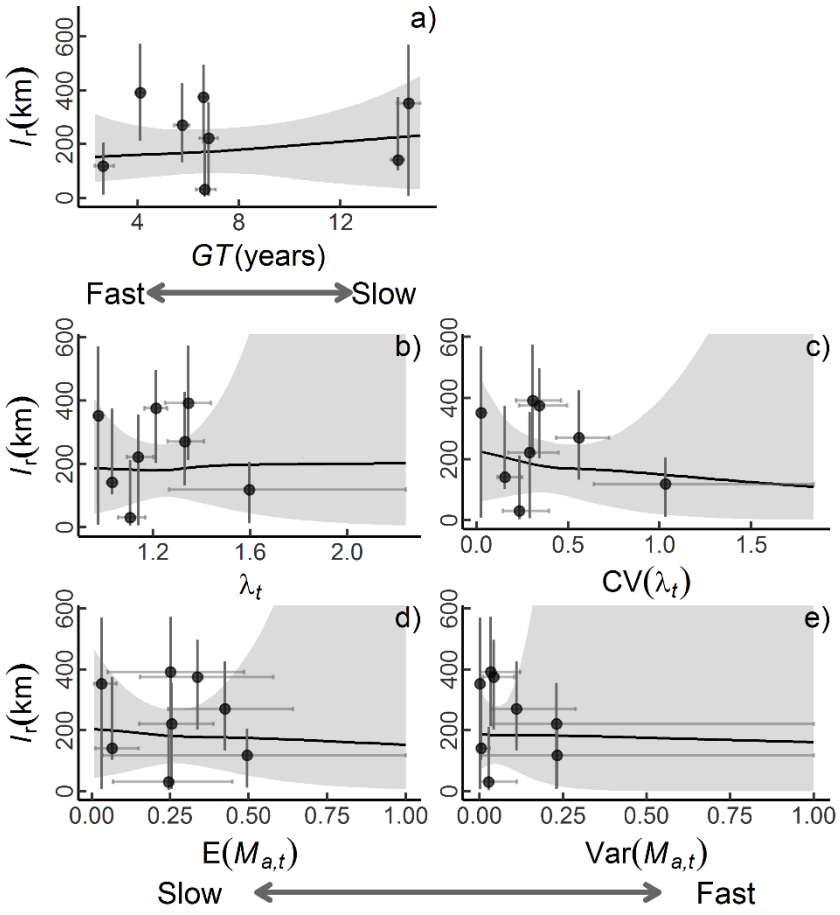


*Figure 3. Relationship between spatial scaling of annual changes in abundance, $l_r$, and a) generation time, $GT$, b) multiplicative population growth rate, $\lambda_t$, c) CV of the multiplicative population growth rate, $CV(\lambda_t)$, d) expected mortality rate, $E(M_{a,t})$ and e) variance of mortality, $Var(M_{a,t})$. Points represent the median of each species' spatial scaling estimates and their estimated life history traits, with the vertical and horizontal lines indicate their 95% confidence intervals and credible intervals, respectively. The regression line shows the model's prediction*

*with the uncertainty shown by the 95% credible sets in grey. The arrow under the x axis indicates the direction of the relationship between the life history traits and the slow-fast continuum.*

## DISCUSSION

Our results show that among species variation in the spatial scaling of abundance synchrony is related to life history in a way that follows the slow-fast continuum, where species located at the slow end have greater spatial scaling of abundance. The general relationship between spatial scaling of abundance and life history was robust to variation in the resolution used to calculate spatial synchrony, at least within the resolution margins explored here. Scaling of synchrony in annual change in abundance also varied with resolution, but was not found to depend on life history parameters under any of the resolutions analysed. Our findings highlight an important connection between species life histories and spatial population dynamics and suggest that knowledge of a species' life history could give an indication of its expected spatial distribution and synchrony, at least among marine fish species.

The slow-fast continuum is a useful predictor of life history variation in a range of taxa, including birds (Sæther & Bakke 2000), mammals (Oli 2004; van de Kerk *et al.* 2013) and reptiles (Shine & Charnov 1992; Clobert *et al.* 1998). While previous studies have identified a trilateral continuum model with up to five distinct life history strategies among fish species (Winemiller & Rose 1992; King & McFarlane 2003), Bjørkvoll *et al.* (2012) showed how a simple linear continuum could describe life history variation in fish species from the Barents Sea community. Towards the slow end species had low reproduction and mortality, slow population growth and long generation times, while fast-lived species showed contrasting attributes. Our results showed the same pattern, despite our smaller species sample size and a different methodology. Furthermore, our findings expand our understanding of life history

401 covariation patterns by showing that the spatial scale of synchrony in abundance within a
402 population correlates with the slow-fast continuum.
403
404 Although the main factors causing spatial synchrony (i.e. dispersal, environmental forcing and
405 trophic interactions) are well documented across taxa (e.g. Hanski & Woiwod 1993; Koenig
406 2001; Grøtan *et al.* 2005; Frank *et al.* 2016), little is known about how a species' pace of life
407 influences these factors. Theoretical studies have proposed mechanisms to link spatial scaling
408 to species traits in ways that are consistent with the general pattern shown empirically here.
409 Lande *et al.* (1999) showed with the general formula $l_\rho^2 = l_e^2 + {ml^2}/{\gamma}$ that a population's spatial
410 scale of synchrony in abundance ($l_\rho^2$) depends on the spatial scale of environmental synchrony
411 ($l_e^2$), individual dispersal rate ($m$), and dispersal distance ($l^2$), but that the contribution of
412 dispersal could be regulated by the strength of density regulation ($\gamma$), which is correlated with
413 pace of life (Beddington & May 1977; Herrando-Pèrez *et al.* 2012). This idea was further
414 developed to allow for higher environmental noise (Engen 2017), showing that individuals from
415 species with lower population growth rates or weaker density regulated populations, such as
416 those towards the slow end of the slow-fast continuum, are expected to disperse farther,
417 allowing them to contribute significantly more to synchrony over larger distances. Other
418 simulation studies have also shown that slower population growth rate and lower reproductive
419 rates increased the relative contribution of dispersal to synchrony, allowing synchrony in
420 population dynamics to extend beyond the one generated by the environment (Söndgerath &
421 Schröder 2002; Ranta *et al.* 2006; Bahn *et al.* 2008). Given the known associations that traits
422 like density regulation, reproductive rate or growth rate have within the slow fast continuum
423 (Herrando-Pèrez *et al.* 2012), it makes sense that a pattern of covariation between the pace
424 of life and spatial scaling exists.
425
426 Results from previous studies on wild populations that included both measurements of spatial
427 population dynamics and of a life history trait provide some support to the reported pattern.

Without making reference to spatial autocorrelation, Kuo *et al.* (2016) showed that slower lived fish species tended to be more homogeneously distributed in space compared to fast lived ones, and hypothesized that greater resistance to stochastic events of slow lived species may be responsible for the pattern (Johst & Brandl 1997). Similarly, a study on British bird populations found that larger body size correlated positively but not significantly with the rate of synchrony decline with increased distance (Paradis *et al.* 2000), supporting our general pattern. However, when they removed the variation caused by changes in the global population abundance to assess how local factors alone were driving synchrony, the correlation between the variables was negative.

Spatial scaling in the synchrony of annual changes in abundance was not found to be predicted by life history. This could be influenced by several factors, but movement dynamics is likely to be a major driver. Homing behaviour could be affecting the spatial synchrony of changes in abundance (Östman *et al.* 2017), and is also a population characteristic that is not associated with life history. For example, all species studied here migrate annually to spawning grounds and feeding grounds (Olsen *et al.* 2010). While the feeding grounds of some of the species studies might be spatially stable (e.g. haddock, cod), other species have more variable feeding grounds. Capelin tends to move northward to follow the plankton blooms triggered by the melting of the sea ice. However, as the melting rate of the ice varies among years (Fossheim *et al.* 2015), the spatial distribution of capelin will also vary, decoupling the abundance at a given site between subsequent years. In addition, many of the species included in our study tend to be age-segregated in space (Olsen *et al.* 2010). Changes in the age structure of the population, induced by for example harvesting, might therefore cause decreased synchrony among local annual changes in abundance (Kuo *et al.* 2016).

The choice of spatial resolution in the grouping of the data can have significant effects on the resulting patterns (Pearson & Carroll 1999; Dungan *et al.* 2002). Here, the choice of resolution in the spatial synchrony analyses influenced the resulting scaling estimates differently

456 depending on the species, but not the relationship between scaling and life history. In fact, the
457 relationship became clearer with coarser resolution. This phenomenon is known as the
458 “modifiable areal unit problem” (Liebhold *et al.* 2012). Variation in the amount of data available
459 for some species, as well as the omission of zeros during the analyses probably led to greater
460 variation at finer resolutions, which was improved after reaching certain resolutions for each
461 of the species. Moreover, increasing the resolution tended to result in higher estimates of
462 scaling for all species, while the uncertainty in the estimates for some species decreased
463 greatly (e.g. saithe).
464
465 The observed extents of the spatial scaling of synchrony in abundance and its annual variation
466 are comparable to previous studies on fish (Myers *et al.* 1997; Östman *et al.* 2017), and
467 indicate that widely synchronized environmental forces and/or dispersal are acting on the
468 populations (Grenfell *et al.* 1998). Interspecific variation in the intensity of external factors, like
469 harvesting pressure, is also expected to cause variation in synchrony (Frank *et al.* 2016) by
470 for example altering the age/size structure of populations (Jørgensen & Holt 2013; Kuo *et al.*
471 2016). Homing behaviours or diet preferences could also influence the dispersal patterns of
472 the species studied differently affecting their synchrony, where food generalists might not need
473 to search as much as specialists, thereby decreasing their dispersal (Yaragina & Dolgov
474 2009).
475
476 All the data used in this study were collected by bottom-trawl surveys. It could be argued that
477 bottom trawling is less appropriate for the two pelagic species in our study (capelin and
478 herring) than for the demersal species (McQuinn 2009; Frank *et al.* 2013). However, bottom
479 trawls can be used to monitor the abundance of pelagic species under the assumption that a
480 constant fraction of the population is available in the sampling volume of the trawl (near the
481 bottom) between years. Pelagic fish species, like herring, are often found near the bottom in
482 shelf areas like the Barents Sea and the North Sea. Therefore, bottom trawl surveys have
483 been used in the stock assessments of for example North Sea herring (see e.g. ICES 2018).

Our results have important implications under future climate change scenarios. Recent publications have predicted that climate change and associated ecological processes (e.g. increased competition or predation) will change population life histories and spatial distributions (Swain *et al.* 2015; Pinceel *et al.* 2016; Lancaster *et al.* 2017). In addition, climate change and other anthropogenic disturbances that alter population cycles, such as harvesting, have been shown to influence the spatial synchrony of populations, with uncertain consequences for their future (Bjørnstad 2000; Vasseur & Fox 2009; Defriez *et al.* 2016; Shestakova *et al.* 2016). Understanding the link between the two processes, and what additional factors could influence spatial synchrony (e.g. geography of synchrony, (Walter *et al.* 2017)), should be a priority within spatial ecology. Although the current study shows quite a clear pattern between life history and spatial scaling of abundance it is based on a limited number of species. It will therefore be important to follow this up with further empirical studies of this pattern, both in the marine environment and among a variety of taxa and ecosystems.

Despite there not being a single mechanism able to explain spatial patterns across scales (Levin 1992), we present a robust pattern that describes how spatial synchrony in population dynamics varies with distance based on the species' pace of life. This relationship helps to bridge knowledge gaps associated with spatial scaling to life history, thereby facilitating a better understanding of population dynamics and potential vulnerabilities associated to their spatial distributions. We encourage the testing of this pattern in other species groups to clarify its generality across ecosystems. Given current ecological challenges, like habitat fragmentation, climate driven invasions or disease outbreaks, the presented pattern could provide important guidelines for future harvesting and conservation strategies.

## Acknowledgements

We are grateful to Eirin Bjørkvoll for facilitating access to the raw results of her paper and providing assistance in their use. In addition, J.F.M. would like to thank Stefan Vriend for all the support and advice. Lastly, we are grateful to James Thorson and two anonymous referees for providing valuable comments in an early version of the paper that we included into the final work. This study was funded by the Research Council of Norway through the Centre of Excellence (project 223257) and research project SUSTAIN (244647).

516 **Bibliography**

517 Aanes, S., Engen, S., Sæther, B.-E. & Aanes, R. (2007). Estimation of the parameters of fish
518 stock dynamics from catch-at-age data and indices of abundance: can natural and fishing
519 mortality be separated? *Can. J. Fish. Aquat. Sci.*, 64, 1130–1142.

520 Aanes, S. & Vølstad, J.H. (2015). Efficient statistical estimators and sampling strategies for
521 estimating the age composition of fish. *Can. J. Fish. Aquat. Sci.*, 72, 938–953.

522 Aglen, A. (1996). Impact of fish distribution and species composition on the relationship
523 between acoustic and swept-area estimates of fish density. *ICES J. Mar. Sci.*, 53, 501–
524 505.

525 Bahn, V., Krohn, W.B. & O'Connor, R.J. (2008). Dispersal leads to spatial autocorrelation in
526 species distributions: A simulation model. *Ecol. Modell.*, 213, 285–292.

527 Barraquand, F. & Murrell, D.J. (2012). Intense or spatially heterogeneous predation can select
528 against prey dispersal. *PLoS One*, 7, e28924.

529 Beddington, J.R. & May, R.M. (1977). Harvesting natural populations in a randomly fluctuating
530 environment. *Science (80-. ).*, 197, 463–465.

531 Bjørkvoll, E., Grøtan, V., Aanes, S., Sæther, B.-E., Engen, S. & Aanes, R. (2012). Stochastic
532 population dynamics and life-history variation in marine fish species. *Am. Nat.*, 180, 372–
533 387.

534 Bjørnstad, O.N. (2000). Cycles and synchrony: two historical 'experiments' and one
535 experience. *J. Anim. Ecol.*, 69, 869–873.

536 Bjørnstad, O.N. & Bolker, B. (2000). Canonical functions for dispersal-induced synchrony.
537 *Proc. R. Soc. B Biol. Sci.*, 267, 1787–1794.

538 Bjørnstad, O.N., Ims, R.A. & Lambin, X. (1999). Spatial population dynamics: analyzing
539 patterns and processes of population synchrony. *Trends Ecol. Evol.*, 14, 427–432.

540 Clobert, J., Garland Jr., T. & Barbault, R. (1998). The evolution of demographic tactics in
541 lizards: a test of some hypotheses concerning life history evolution. *J. Evol. Biol.*, 11,
542 329–364.

543 Cressie, N. & Wikle, C.K. (2011). *Statistics for spatio-temporal data*. John Wiley & Sons, New

544 Jersey.
545 Defriez, E.J., Sheppard, L.W., Reid, P.C. & Reuman, D.C. (2016). Climate change-related
546 regime shifts have altered spatial synchrony of plankton dynamics in the North Sea. *Glob.*
547 *Chang. Biol.*, 22, 2069–2080.
548 Dungan, J.L., Perry, J.N., Dale, M.R.T., Legendre, P., Citron-Pousty, S., Fortin, M.J., *et al.*
549 (2002). A balanced view of scale in spatial statistical analysis. *Ecography (Cop.).*, 25,
550 626–640.
551 Ellis, J. & Schneider, D.C. (2008). Spatial and temporal scaling in benthic ecology. *J. Exp.*
552 *Mar. Bio. Ecol.*, 366, 92–98.
553 Engen, S. (2007). Stochastic growth and extinction in a spatial geometric Brownian population
554 model with migration and correlated noise. *Math. Biosci.*, 209, 240–255.
555 Engen, S. (2017). Spatial synchrony and harvesting in fluctuating populations: Relaxing the
556 small noise assumption. *Theor. Popul. Biol.*, 116, 18–26.
557 Engen, S., Cao, F.J. & Sæther, B. (2018). The effect of harvesting on the spatial synchrony of
558 population fluctuations. *Theor. Popul. Biol.*, 123, 28–34.
559 Engen, S., Lande, R., Sæther, B.-E. & Weimerskirch, H. (2005a). Extinction in relation to
560 demographic and environmental stochasticity in age-structured models. *Math. Biosci.*,
561 195, 210–227.
562 Engen, S., Lande, R. & Sæther, B. (2002). The spatial scale of population fluctuations and
563 quasi-extinction risk. *Am. Nat.*, 160, 439–451.
564 Engen, S., Lande, R., Seæther, B.E. & Bregnballe, T. (2005b). Estimating the pattern of
565 synchrony in fluctuating populations. *J. Anim. Ecol.*, 74, 601–611.
566 Fauchald, P., Mauritzen, M. & Gjøsæter, H. (2006). Density-dependent migratory waves in the
567 marine pelagic ecosystem. *Ecology*, 87, 2915–2924.
568 Ferguson, S.H. & Lariviere, S. (2002). Can comparing life histories help conserve carnivores?
569 *Anim. Conserv.*, 5, 1–12.
570 Fossheim, M., Primicerio, R., Johannesen, E., Ingvaldsen, R.B., Aschan, M.M. & Dolgov, A.
571 V. (2015). Recent warming leads to a rapid borealization of fish communities in the Arctic.

572 *Nat. Clim. Chang.*, 5, 1–6.
573 Frank, K.T., Leggett, W.C., Petrie, B.D., Fisher, J.A.D., Shackell, N.L. & Taggart, C.T. (2013).
574 Irruptive prey dynamics following the groundfish collapse in the Northwest Atlantic: an
575 illusion? *ICES J. Mar. Sci.*, 70, 1299–1307.
576 Frank, K.T., Petrie, B., Leggett, W.C. & Boyce, D.G. (2016). Large scale, synchronous
577 variability of marine fish populations driven by commercial exploitation. *Proc. Natl. Acad.*
578 *Sci.*, 113, 8248–8253.
579 Giometto, A., Altermatt, F. & Rinaldo, A. (2017). Demographic stochasticity and resource
580 autocorrelation control biological invasions in heterogeneous landscapes. *Oikos*, 126,
581 1554–1563.
582 Grenfell, B.T., Wilson, K., Finkenstädt, B.F., Coulson, T.N., Murray, S., Albon, S.D., *et al.*
583 (1998). Noise and determinism in synchronized sheep dynamics. *Nature*, 394, 674–677.
584 Grøtan, V., Sæther, B.-E., Engen, S., Solberg, E.J., Linnell, J.D., Andersen, R., *et al.* (2005).
585 Climate causes large-scale spatial synchrony in population fluctuations of a temperature
586 herbivore. *Ecology*, 86, 1472–1482.
587 Hanski, I. & Woiwod, I.P. (1993). Spatial synchrony in the dynamics of moth and aphid
588 populations. *J. Anim. Ecol.*, 62, 656.
589 Heino, M., Kaitala, V., Ranta, E. & Lindström, J. (1997). Synchronous dynamics and rates of
590 extinction in spatially structured populations. *Proc. R. Soc. London B Biol. Sci.*, 264, 481–
591 486.
592 Herrando-Pèrez, S., Delean, S., Brook, B.W. & Bradshaw, C.J.A. (2012). Strength of density
593 feedback in census data increases from slow to fast life histories. *Ecol. Evol.*, 2, 1922–
594 1934.
595 Huse, G. (2016). A spatial approach to understanding herring population dynamics. *Can. J.*
596 *Fish. Aquat. Sci.*, 73, 177–188.
597 ICES. (2008a). *Report of the Arctic Fisheries Working Group (AFWG)*. Copenhagen,
598 Denmark.
599 ICES. (2008b). *Report of the Working Group on Widely Distributed Stocks (WGWIDE)*.

Copenhagen, Denmark.

ICES. (2009). *Report of the Arctic Fisheries Working Group (AFWG)*. San Sebastian, Spain.

ICES. (2016). Ecosystem overviews: Barents Sea Ecoregion. *ICES Advice 2016, B. 9*, 8.

ICES. (2018). *Report of the Herring Assessment Working Group for the Area South of 62°N (HAWG)*. ICES HQ, Copenhagen, Denmark.

Ims, R.A. & Andreassen, H.P. (2000). Spatial synchronization of vole population dynamics by predatory birds. *Nature*, 408, 194–196.

Jakobsen, T., Korsbrekke, K., Mehl, S. & Nakken, O. (1997). Norwegian combined acoustic and bottom trawl surveys for demersal fish in the Barents Sea during winter. *ICES*, N: 17, 26.

Jennings, S., Reynolds, J.D. & Mills, S.C. (1998). Life history correlates of responses to fisheries exploitation. *Proc. R. Soc.*, 265, 333–339.

Johannesen, E., Wenneck, T.D.L., Høines, Å., Aglen, A., Mehl, S., Mjanger, H., *et al.* (2009). Egner vintertoktet seg til overvåking av endringer i fiskesamfunnet i Barentshavet? : en gjennomgang av metodikk og data fra 1981-2007, 29.

Johst, K. & Brandl, R. (1997). Body Size and Extinction Risk in a Stochastic Environment. *Oikos*, 78, 612.

Jones, J., Doran, P.J. & Holmes, R.T. (2007). Spatial scaling of avian population dynamics: Population abundance, growth rate, and variability. *Ecology*, 88, 2505–2515.

Jones, O.R., Gaillard, J.M., Tuljapurkar, S., Alho, J.S., Armitage, K.B., Becker, P.H., *et al.* (2008). Senescence rates are determined by ranking on the fast-slow life-history continuum. *Ecol. Lett.*, 11, 664–673.

Jørgensen, C. & Holt, R.E. (2013). Natural mortality: Its ecology, how it shapes fish life histories, and why it may be increased by fishing. *J. Sea Res.*, 75, 8–18.

Kausrud, K.L., Viljugrein, H., Frigessi, A., Begon, M., Davis, S., Leirs, H., *et al.* (2007). Climatically driven synchrony of gerbil populations allows large-scale plague outbreaks. *Proc. R. Soc. B Biol. Sci.*, 274, 1963–1969.

Kendall, B.E., Bjørnstad, O.N., Bascompte, J., Keitt, T.H. & Fagan, W.F. (2000). Dispersal,

628 Environmental Correlation, and Spatial Synchrony in Population Dynamics. *Am. Nat.*,
629 155, 628–636.
630 van de Kerk, M., de Kroon, H., Conde, D.A. & Jongejans, E. (2013). Carnivora population
631 dynamics are as slow and as fast as those of other mammals: Implications for their
632 conservation. *PLoS One*, 8, e70354.
633 King, J.R. & McFarlane, G.A. (2003). Marine fish life history strategies: applications to fishery
634 management. *Fish. Manag. Ecol.*, 10, 249–264.
635 Koenig, W.D. (1999). Spatial autocorrelation of ecological phenomena. *Trends Ecol. Evol.*, 14,
636 22–26.
637 Koenig, W.D. (2001). Spatial autocorrelation and local disappearances in winter north
638 american birds. *Ecology*, 82, 2636–2644.
639 Kuo, T.C., Mandal, S., Yamauchi, A. & Hsieh, C.H. (2016). Life history traits and exploitation
640 affect the spatial mean-variance relationship in fish abundance. *Ecology*, 97, 1251–1259.
641 Lancaster, L.T., Morrison, G. & Fitt, R.N. (2017). Life history trade-offs, the intensity of
642 competition, and coexistence in novel and evolving communities under climate change.
643 *Philos. Trans. R. Soc. B Biol. Sci.*, 372.
644 Lande, R., Engen, S. & Sæther, B.-E. (1999). Spatial scale of population synchrony:
645 Environmental correlation versus dispersal and density regulation. *Am. Nat.*, 154, 271–
646 281.
647 Levin, S.A. (1992). The problem of pattern and scale in ecology. *Ecology*, 73, 1943–1967.
648 Liebhold, A., Koenig, W.D. & Bjørnstad, O.N. (2004). Spatial synchrony in population
649 dynamics. *Annu. Rev. Ecol. Evol. Syst.*, 35, 467–490.
650 Liebhold, A.M., Haynes, K.J. & Bjørnstad, O.N. (2012). Spatial Synchrony of Insect Outbreaks.
651 In: *Insect Outbreaks Revisited*. John Wiley & Sons, Ltd, Chichester, UK, pp. 113–125.
652 Lindström, J., Ranta, E. & Lindén, H. (1996). Large-scale synchrony in the dynamics of
653 capercaillie, black grouse and hazel grouse populations in Finland. *Oikos*, 76, 221–227.
654 McQuinn, I.H. (2009). Pelagic fish outburst or suprabenthic habitat occupation: legacy of the
655 Atlantic cod (Gadus morhua) collapse in eastern Canada. *Can. J. Fish. Aquat. Sci.*, 66,

2256–2262.

Moran, P. (1953). The statistical analysis of the Canadian lynx cycle. II. Synchronization and meteorology. *Aust. J. Zool.*, 1, 291–298.

Murdoch, W.W., Briggs, C.J., Nisbet, R.M. & Stewart-Oaten, A. (1992). Aggregation and Stability in Metapopulation Models. *Am. Nat.*, 140, 41–58.

Myers, R.A., Mertz, G. & Bridson, J. (1997). Spatial scales of interannual recruitment variations of marine, anadromous, and freshwater fish. *Can. J. Fish. Aquat. Sci.*, 54, 1400–1407.

Oli, M.K. (2004). The fast–slow continuum and mammalian life-history patterns: an empirical evaluation. *Basic Appl. Ecol.*, 5, 449–463.

Olsen, E., Aanes, S., Mehl, S., Holst, J.C., Aglen, A. & Gjøsæter, H. (2010). Cod, haddock, saithe, herring, and capelin in the Barents Sea and adjacent waters: A review of the biological value of the area. *ICES J. Mar. Sci.*, 67, 87–101.

Östman, Ö., Olsson, J., Dannewitz, J., Palm, S. & Florin, A.B. (2017). Inferring spatial structure from population genetics and spatial synchrony in demography of Baltic Sea fishes: implications for management. *Fish Fish.*, 18, 324–339.

Ovaskainen, O. & Cornell, S.J. (2006). Space and stochasticity in population dynamics. *Proc. Natl. Acad. Sci.*, 103, 12781–12786.

Paradis, E., Baillie, S.R., Sutherland, W.J. & Gregory, R.D. (1999). Dispersal and spatial scale affect synchrony in spatial population dynamics. *Ecol. Lett.*, 2, 114–120.

Paradis, E., Baillie, S.R., Sutherland, W.J. & Gregory, R.D. (2000). Spatial synchrony in populations of birds: Effects of habitat, population trend, and spatial scale. *Ecology*, 81, 2112.

Pearson, D.L. & Carroll, S.S. (1999). The influence of spatial scale on cross-taxon congruence patterns and prediction accuracy of species richness. *J. Biogeogr.*, 26, 1079–1090.

Pennington, M., Shevelev, M.S., Vølstad, J.H. & Nakken, O. (2011). Bottom trawl surveys. In: *The Barents Sea: ecosystem, resources, management: Half a century of Russian-Norwegian cooperation* (ed. Jakobsen, T. et al.). Tapir Academic Press, Trondheim, pp. 570–583.

684 Pinceel, T., Vanschoenwinkel, B., Brendonck, L. & Buschke, F. (2016). Modelling the
685 sensitivity of life history traits to climate change in a temporary pool crustacean. *Sci. Rep.*,
686 6, 1–5.
687 R Core Team. (2018). *R: A language and environment for statistical computing*. R Foundation
688 for Statistical Computing, Vienna, Austria.
689 Ranta, E. (1997). The Spatial Dimension in Population Fluctuations. *Science (80-. ).*, 278,
690 1621–1623.
691 Ranta, E., Lundberg, P. & Kaitala, V. (2006). *Ecology of Populations*. Cambridge University
692 Press, Cambridge.
693 Royama, T. (1977). Population persistence and density dependence. *Ecol. Monogr.*, 47, 1–
694 35.
695 Ruokolainen, L. (2013). Spatio-temporal environmental correlation and population variability
696 in simple metacommunities. *PLoS One*, 8, e72325.
697 Sæther, B.-E. (1997). Environmental stochasticity and population dynamics of large
698 herbivores: A search for mechanisms. *Trends Ecol. Evol.*, 12, 143–147.
699 Sæther, B.-E. & Bakke, O. (2000). Avian Life History Variation and Contribution of
700 Demographic Traits to the Population Growth Rate. *Ecology*, 81, 642.
701 Sæther, B.-E., Engen, S., Grøtan, V., Fiedler, W., Matthysen, E., Visser, M.E., *et al.* (2007).
702 The extended Moran effect and large-scale synchronous fluctuations in the size of great
703 tit and blue tit populations. *J. Anim. Ecol.*, 76, 315–325.
704 Sæther, B.-E., Ringsby, T.H., Røskaft, E., Saether, B.-E. & Roskaft, E. (1996). Life history
705 variation, population processes and priorities in species conservation: Towards a reunion
706 of research paradigms. *Oikos*, 77, 217–226.
707 Shelton, A.O. & Mangel, M. (2011). Fluctuations of fish populations and the magnifying effects
708 of fishing. *Proc. Natl. Acad. Sci.*, 108, 7075–7080.
709 Shestakova, T.A., Gutiérrez, E., Kirdyanov, A. V., Camarero, J.J., Génova, M., Knorre, A.A.,
710 *et al.* (2016). Forests synchronize their growth in contrasting Eurasian regions in
711 response to climate warming. *Proc. Natl. Acad. Sci.*, 113, 662–667.

712 Shine, R. & Charnov, E.L. (1992). Patterns of survival, growth, and maturation in snakes and
713 lizards. *Am. Nat.*, 139, 1257–1269.
714 Söndgerath, D. & Schröder, B. (2002). Population dynamics and habitat connectivity affecting
715 the spatial spread of populations - A simulation study. *Landsc. Ecol.*, 17, 57–70.
716 Stiansen, J.E., Filin, A.A. & (editors). (2008). *Joint PINRO/IMR Report on the state of the*
717 *Barents Sea ecosystem in 2007, with expected situation and considerations for*
718 *Management*. *IMR-PINRO Jt. Rep. Ser. 2008(1)*. Bergen, Norway.
719 Swain, D.P., Benoît, H.P. & Hammill, M.O. (2015). Spatial distribution of fishes in a Northwest
720 Atlantic ecosystem in relation to risk of predation by a marine mammal. *J. Anim. Ecol.*,
721 84, 1286–1298.
722 Thorson, J.T., Munch, S.B., Cope, J.M. & Gao, J. (2017). Predicting life history parameters for
723 all fishes worldwide. *Ecol. Appl.*, 27, 2262–2276.
724 Vasseur, D.A. & Fox, J.W. (2009). Phase-locking and environmental fluctuations generate
725 synchrony in a predator-prey community. *Nature*, 460, 1007–1010.
726 Walter, J.A., Sheppard, L.W., Anderson, T.L., Kastens, J.H., Bjørnstad, O.N., Liebhold, A.M.,
727 *et al.* (2017). The geography of spatial synchrony. *Ecol. Lett.*, 20, 801–814.
728 Winemiller, K.O. & Rose, K.A. (1992). Patterns of life-history diversification in North American
729 fishes: implications for population regulation. *Can. J. Fish. Aquat. Sci.*, 49, 2196–2218.
730 Yaragina, N.A. & Dolgov, A. V. (2009). Ecosystem structure and resilience-A comparison
731 between the Norwegian and the Barents Sea. *Deep. Res. Part II Top. Stud. Oceanogr.*,
732 56, 2141–2153.
733